Performance, Heating, and Current Drive Scenarios of ASDEX Upgrade Advanced Tokamak Discharges

R. C. Wolf[1], J. Hobirk[1], G. Conway[1], O. Gruber[1], A. Gude[1], S. Günter[1], K. Kirov[1], B. Kurzan[1], M. Maraschek[1], P. J. Mc Carthy[2], H. Meister[1], F. Leuterer[1], G. V. Pereverzev[1], E. Poli[1], F. Ryter[1], and the ASDEX Upgrade Team

[1]Max-Planck-Institut für Plasmaphysik, EURATOM-Association, D-85748 Garching
[2]Physics Department, University College Cork, Association Euratom-DCU, Cork, Ireland

e-mail contact of main author: robert.wolf@ipp.mpg.de

Abstract. Various approaches to high performance and steady state operation are presented. Strong neutral beam heating in the current ramp leads to internal transport barriers (ITBs) in conjunction with negative central magnetic shear. In high β_p discharges full non-inductive current drive has been achieved transiently. At Greenwald density values of β_p=3.1, β_N=2.8, and $H_{ITER89-P}$=1.8 have been reached simultaneously. In plasmas with ITBs and L-mode edge additional electron cyclotron resonance heating (ECRH) and current drive (ECCD) facilitates high core confinement with $T_e \approx T_i$. Central ECCD has been applied in low density, low current discharge. For ECCD in co-current direction a current drive fraction of 82% is calculated. In case of counter-ECCD negative central shear with q_{min}>1 leads to the formation of an electron ITB.

1. Introduction

Research in the field of advanced tokamak scenarios aims to develop an operating regime with improved confinement and stability properties, thus allowing a reduced size tokamak reactor to be operated in steady state [1, 2, 3, 4, 5]. Low or even negative central magnetic shear facilitates the formation of internal transport barriers (ITBs), characterized by large pressure gradients in the region of reduced plasma turbulence. Thus, in addition to the larger energy content in the plasma core, the intrinsic bootstrap current, which is generated by the pressure gradient, can constitute a significant part of the plasma current. For steady state operation the inductive or ohmic plasma current has to be completely replaced. In addition to the bootstrap current, this usually requires an externally driven current, which however should be kept low to minimize the re-circulating energy in a tokamak reactor. Common current drive techniques are the injection of fast particle by neutral beams [6], or of electromagnetic waves. The latter includes electron cyclotron current drive (ECCD), which heats the electrons by resonant absorption and produces a toroidal current by launching the electromagnetic waves in toroidal direction. Recently it has been shown, that ECCD can be used to produce steady state fully non-inductive current drive in a tokamak plasma [7].

Here, we first report on recent progress made in ASDEX Upgrade ITB plasmas with predominantly ion heating. Secondly we present H-mode discharges with high poloidal β [8, 9], and in the final part heating and current drive scenarios by means of ECCD are discussed.

2. High ion temperature regimes

Improved core confinement or internal transport barriers for the plasma ions have been attained in various tokamak experiments by strong ion heating in combination with low or negative central magnetic shear [1, 2, 10, 4, 11]. Without sufficient external current drive, a common technique to establish shear reversal is to increase the electron temperature during the current ramp by auxiliary heating and hence reduce the current diffusion. In ASDEX Upgrade this is used to generate a variety of q-profiles by modifying the time and level of the heating power during the current ramp. The q-profiles range from monotonic shape with zero magnetic

shear in the plasma core and $q_0 \approx 1$ to negative central shear and $q_{min} > 1$. In the first case fishbones with mode numbers of (m=1,n=1) clamp the current profile by reconnection, preventing the appearance of sawteeth [12, 13]. Thus, improved stability and confinement could be combined, reaching stationary values of $H_{ITER89-P}$=3.0 and β_N=2.4 in plasmas with H-mode edge. In discharges with contact to the inner wall, where the heating power applied during the current ramp is increased [14, 15], the central magnetic shear becomes transiently negative and strong internal transport barriers form. In ASDEX Upgrade the H-mode transition

has to be avoided in these plasmas, as the edge bootstrap current associated with the H-mode, in combination with the large pressure gradients of the ITB, results in the destabilization of an external kink mode as soon as the edge q becomes rational.

The negative central shear regime in AS-DEX Upgrade has been extended by upper single null (SN) configurations. This allows higher power levels than in the limiter discharges and simultaneously an increased H-mode threshold due to the reversal of the ion ∇B drift. In figure 1 temperature and q profiles of an early and later phase of an ITB development are shown. The q-values have been inferred by the equilibrium code CLISTE [16] using motional Stark effect (MSE) measurements [17]. At 0.65s q_{min} is still above two and the ITB is restricted to a small plasma volume. Increasing the power to 7.5MW, the temperatures rise and the radius of the ITB expands. This is associated also with an outward shift of the q_{min} radius.

Shortly before the disruptive termination of the discharge an H-mode transition occurs. As described above, an ideal mode, here with (m=5,n=2), develops which couples to an external kink [18] when q_{95} approaches 4, finally causing the disruption.
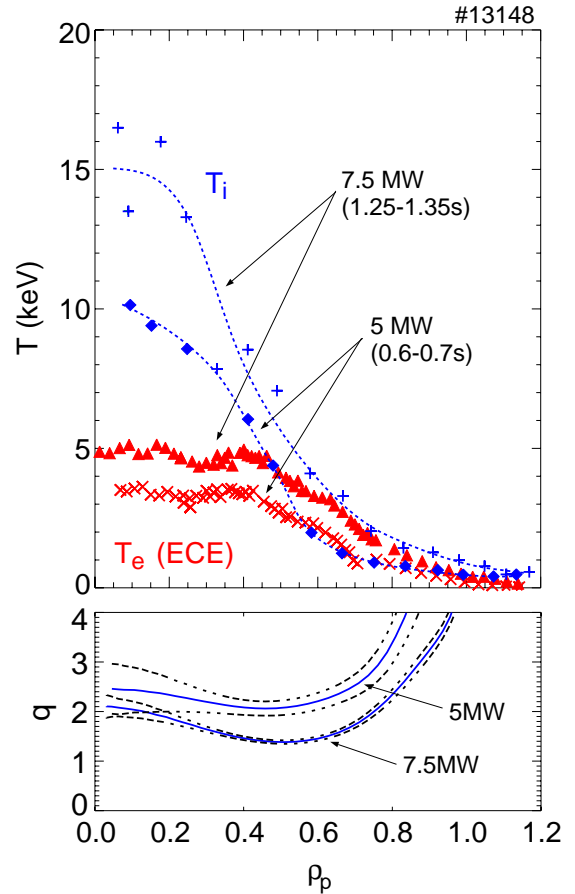

Figure 1. Temperature (T_i from charge exchange recombination spectroscopy (CXRS), T_e from electron cyclotron emission (ECE)) and q-profiles of discharge #13148. Comparing the 5MW phase at 0.65s with the 7.5MW phase at 1.3s, the increase of the power leads to an expansion of the q_{min} radius and the ITB.

3. High β_p discharges

In order to reduce the inductively driven current in a tokamak plasma, a large fraction of the bootstrap current, which is generated by the pressure gradient, is desirable. To achieve this, the poloidal β is maximized by operating at a low plasma current and sufficiently high heating power [8, 9].

In ASDEX Upgrade at 400kA plasma current, 2T toroidal magnetic field, and up to 10MW of neutral beam power, values of β_p above 3 in H-mode plasmas have been attained. The time traces of the major plasma parameters of such discharges are shown in figure 2. The

density rise initially is facilitated by edge gas fuelling. Above 7.5MW of NBI this is no longer required to maintain the density at or above $\overline{n_e}/n_G = 1$, which could be an indication for improved particle confinement. In figure 3 the temperature profiles and the corresponding β-values, H-factors ($H_{ITER89\text{-}P}$), and normalized densities of discharge #13741 at two time points are presented. Figure 3(a) shows the low power phase with 2.5MW NBI. After 2.1s,
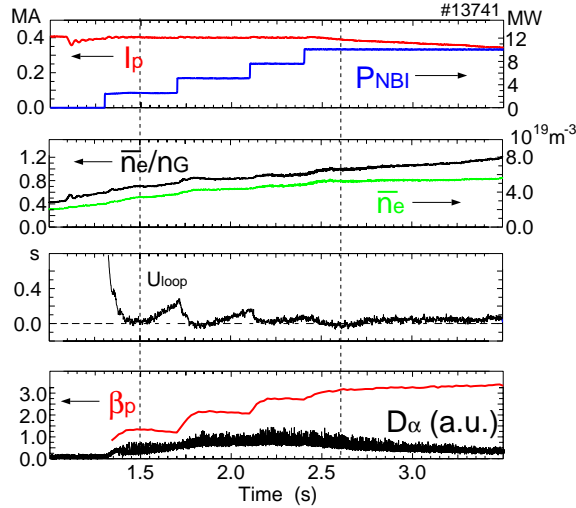

Figure 2. Time evolution of high β_p discharge. Shown are plasma current (I_p), neutral beam power (P_{NBI}), line averaged and fraction of Greenwald density ($\overline{n_e}$, $\overline{n_e}/n_G$), loop voltage (U_{loop}), divertor D_α-signal, and poloidal β (β_p). P_{NBI} is stepped up to 10MW. The current in the ohmic transformer is kept constant from 2.5s onwards.

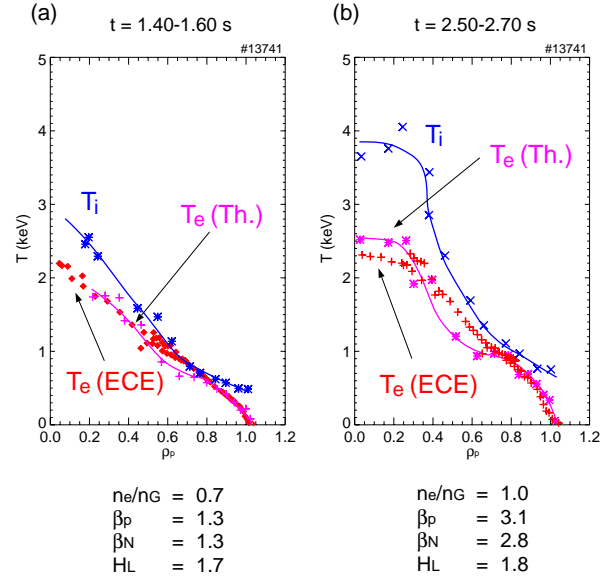| (a) t = 1.40-1.60 s	(b) t = 2.50-2.70 s
n_e/n_G = 0.7	n_e/n_G = 1.0
β_p = 1.3	β_p = 3.1
β_N = 1.3	β_N = 2.8
H_L = 1.7	H_L = 1.8

Figure 3. Temperature profiles at two time points of discharge #13741, averaged over 200ms respectively. In (a) only 2.5MW of NBI is applied. In (b), when P_{NBI} exceeds 7.5MW, in particular the ion temperature (T_i) exhibits a strong reduction of the gradient length at $\rho_p=0.4$. For the electrons (T_e), both, Thomson scattering and ECE measurements are shown. The performance is expressed in terms of Greenwald density (n_e/n_G), normalized β (β_N), poloidal β (β_p), and H-factor relative to L-mode scaling ($H_L=H_{ITER89\text{-}P}$).

when the beam power increases to 7.5MW, the sawtooth activity disappears and the gradient length of the ion temperature decreases strongly in the vicinity of $\rho_p=0.4$, while in the plasma center a plateau is formed. In figure 3(b) the ion and electron   temperatures are shown after the power has been increased to 10MW. The radially changing gradient length of T_i bears the resemblance to ion internal transport barrier observed in ASDEX Upgrade reversed shear plasmas. The line averaged density, in contrast, in absolute terms is higher by 40% and expressed in Greenwald density by almost a factor of 4. The appearance of this ITB coincides with the extinction of the sawtooth activity. Similar to the improved confinement H-mode [13], in which the stationarity of the current profile is explained by fishbone driven reconnection [12], (m=1, n=1) fishbones remain in the plasma, indicating that a q=1 surface is still present. In figure 4 the time points before and after the ITB formation, shown in figure 3(a) and (b), are compared with respect to their ion thermal conductivities, which have been calculated using the transport code ASTRA [19]. Despite the fourfold increase of the heating power, χ_i is lower in the high power phase at 2.6s except in the very plasma center where the temperature plateau is formed. In particular at the ITB location, due to the steepening of the T_i-gradient, χ_i decreases by more then a factor of two from about 1.3m^2/s to 0.5m^2/s. For

the computation of the neoclassical χ, models with and without finite orbit width correction have been used [20, 21]. In addition to the decrease of χ_i in the progression of the discharge, χ_{neo} increases, which is caused by the density rise. Hence, χ_i becomes neoclassical or even drops below that value in the plasma core.
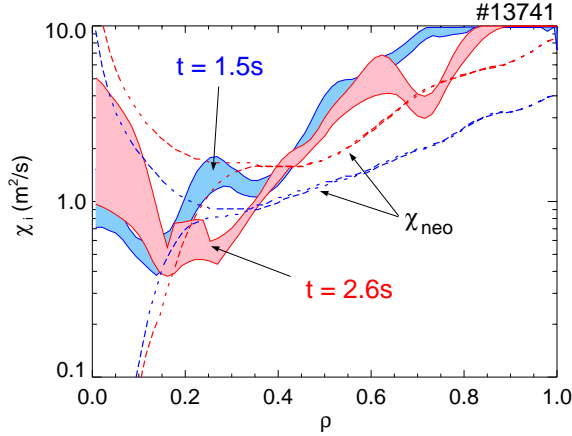

Figure 4. Comparison of the ion thermal conductivity (χ_i) profiles before (1.5s) and after (2.6s) the formation and of the ITB at 2.5MW and 10MW of NBI, respectively. At the ITB location (in this figure the toroidal $\rho \approx 0.25$ corresponds to $\rho_p \approx 0.45$ in figure 3) χ_i drops by a factor of two. The neoclassical ion thermal conductivity (χ_{neo}) increases due to the density rise.

For the investigation of the current composition, the current diffusion model of AS-TRA is employed, which assumes neoclassical conductivity. From the experimental values of T_e and under the assumption that Z_{eff} is constant, the temporal evolution of the radial current distribution is calculated consisting of ohmic, beam driven, and bootstrap current [22]. In figure 5 the current profiles thus obtained are shown. To get an estimate of the uncertainty T_e, has been varied by
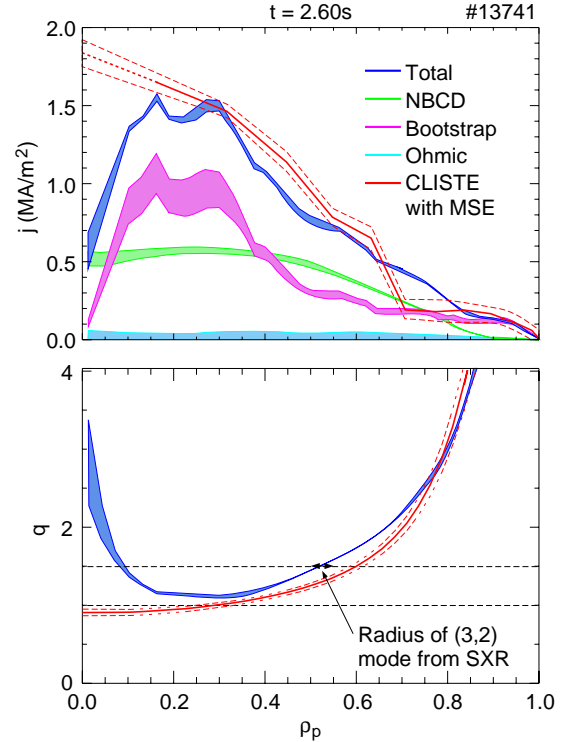

Figure 5. Composition of current profile and q-profile for discharge #13741 at 10MW of NBI calculated with ASTRA. The scatter of the profiles and the resulting uncertainties of the current fractions correspond to variations of T_e by $\pm 10\%$ and Z_{eff} between 1.5 and 3. In the region inside $\rho_p \approx 0.16$, where no MSE data points are available, the corresponding part of the current profile is indicated by a dashed line. For comparison, the (m=3,n=2) mode location from SXR is included.

$\pm 10\%$ and Z_{eff} between 1.5 and 3. The effect on the total current profile is less pronounced than on the individual contributions, which is caused by the different dependencies from these quantities, partly compensating each other. At 1.5s (2.5MW of NBI) the plasma current consists predominantly of the inductive part (f_{OH} = 59%). At 2.6s (10MW of NBI) the plasma current is within the error bars fully non-inductive with a bootstrap current fraction of 56%. This is confirmed by the temporarily negative loop voltage (figure 2). Due to a confinement degradation the bootstrap current and consequently the plasma current decreases after keeping the ohmic transformer at a constant level.

The current or q-profiles, inferred from the MSE measurements utilizing the equilibrium code CLISTE [16], agree reasonably well with ASTRA calculations, confirming the evolution

towards a broader current profile, which is generated mainly by the bootstrap current. Since the heating beam, which is also used for the MSE diagnostic, does not cover regions inside $\rho_p \approx 0.16$, the reversed magnetic shear close to the magnetic axis, predicted by ASTRA (figure 5) and generated by the bootstrap current, cannot be resolved.

4. Electron cyclotron resonance heating and current drive

Electron cyclotron resonance waves facilitate the direct and local heating of the plasma electrons. In addition, toroidal current drive is obtained by launching the waves in toroidal direction. In ASDEX Upgrade the ECRH system [23] consists of four gyrotrons delivering up to 1.6MW. Movable mirrors allow poloidal and toroidal launch angles of the focused ECRH waves to be changed on a shot to shot basis. Thus, in addition to pure electron heating, co- and counter-current can be driven.

Combined ion and electron internal transport barriers

By a combination of NBI during the current ramp to establish negative central magnetic shear and ECCD for electron heating and current drive, ITBs of electrons and ions with $T_e \approx T_i$ have been achieved in ASDEX Upgrade [24, 15]. As the plasma is in contact with the inner wall, the plasma edge remains L-mode like. In figure 6 the time evolution of the central and minimum q, and the electron and ion temperatures are shown. In the NBI only case (figure 6(a)) an ion ITB with a central T_i of about 10keV is formed. The collapse of T_i at 0.65s, when q_{min} reaches two, is caused by the occurrence of a (m=2,n=1) double tearing mode. By applying central counter-ECCD in a similar discharge also an electron ITB occurs, seen as a strong rise of the electron temperature in figure 6(b). Since the ITB is located inside $\rho_p = 0.4$, covering a small fraction of the plasma volume only, the maximum $H_{ITER89-P}$ at 1s in both cases is about 1.8.

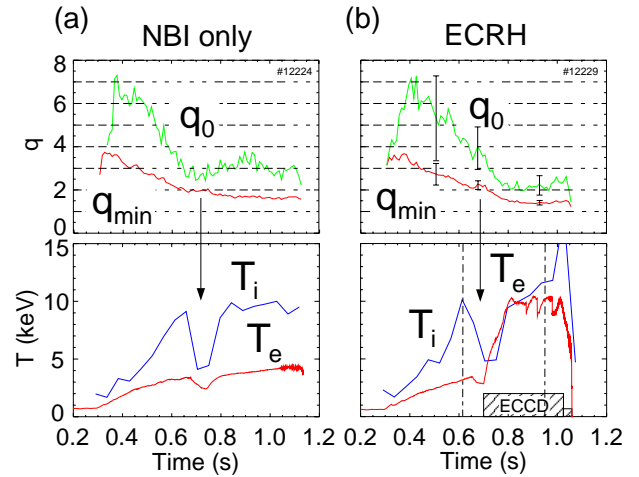*Figure 6. (a) Temporal evolution of central and minimum q (q_0, q_{min}) for a discharge with central reversed magnetic shear ($q_0 > q_{min}$) and internal transport barrier, established by neutral beam heating in the current ramp. (b) With additional central counter-ECCD also the electron temperature can be raised to 10keV without any confinement degradation.*

Electron cyclotron heating and current drive experiments

For the investigation of electron heating and current drive, ECCD has been applied in L-mode plasmas with low current and density. The low density facilitates a high current drive efficiency, which scales with T_e/n_e, since not only n_e is low, but also the electron temperature becomes large. Starting from an ohmic plasma at $\overline{n}_e \approx 1.5 \times 10^{19} m^{-3}$ the electron cyclotron resonance waves of three gyrotrons (1.2MW) were launched in either co- or counter-current direction. The remaining 0.4MW have been used for heating only. Central deposition near the magnetic axis was chosen. In ASDEX Upgrade this requires a toroidal magnetic field of 2.3T.
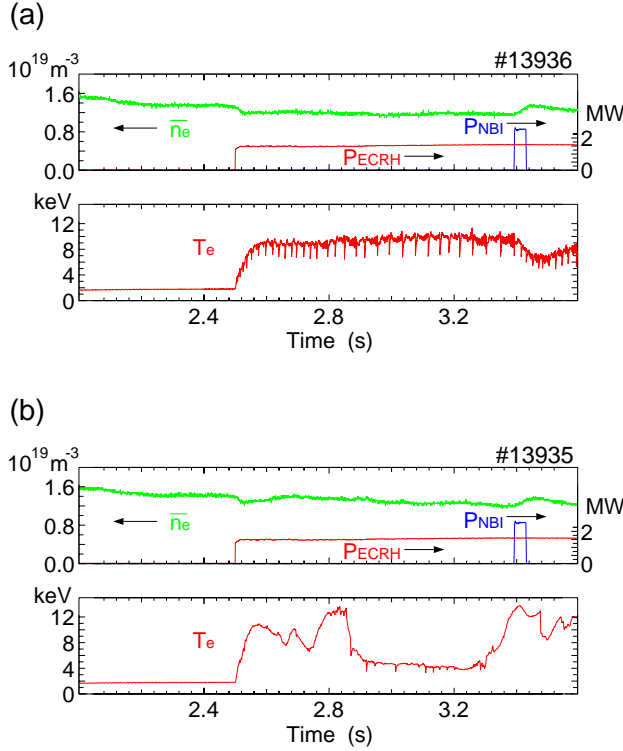
Figure 7. (a) Time evolution of heating power wave forms, line averaged density ($\overline{n}_e$), and central electron temperature (T_e) for discharge #13936. At 2.5s 1.2MW of co-ECCD and 0.4MW of pure ECRH is switched on. (b) The same for discharge #13935, where, instead of co-, counter-ECCD has been applied.

Figure 8. Temperature profiles from ECE and Thomson scattering for (a) the co- and (b) the counter-ECCD discharge. In (a) the T_e-profile is an average over 800ms. In (b), as T_e changes strongly during the ECCD phase, the average is taken over 50ms only. The T_i-profiles from CXRS are measured during the NBI pulse at 3.4s.

In figure 7 the time evolutions of heating power, central electron temperatures, and line averaged densities of the co- and counter-current drive discharges are compared. With the onset of ECRH T_e rises sharply in both cases. However, the temperature profiles are distinctly different (figure 8). While for co-ECCD the temperature gradient in the plasma core does not show a radial variation, an electron internal transport barrier develops in the counter-ECCD discharge.

The current diffusion has been simulated with the ASTRA code taking the evolution of the electron temperature and the ECCD into account. For the electron temperature profile, Thomson scattering and ECE measurements are compared in figure 8. The discrepancy between T_e from ECE and Thomson scattering in the plasma center, in particular for counter-ECCD, indicates that non-thermal parts may be contained in the ECE measurements. However, in the region between ρ_p=0.2 and 0.4, where the gradient length of the electron temperature decreases when going from co- to counter-ECCD, ECE and Thomson scattering measurements agree.

The deposition of the electron cyclotron waves has been calculated with the TORBEAM code [25]. The beam tracing technique [26] is used here to describe the propagation and absorption of the waves, taking into account diffraction effects. At 2.65s the TORBEAM calculations predict a current drive fraction of 82% for co-ECCD, and -80% for counter-ECCD. The ASTRA results (Kadomtsev reconnection [27] is simulated) show that, for co-ECCD, the full electron cyclotron current of 82%, as predicted by TORBEAM, is reached at 3.3s of discharge #13936 after 800ms of ECCD. The remaining part is divided up into 12% bootstrap current and 6% ohmic current fraction. In the counter-ECCD case, convergence problems in the ASTRA equilibrium solver, caused by the strong gradients of the current distribution, did not permit a quantitative assessment of the current fractions.
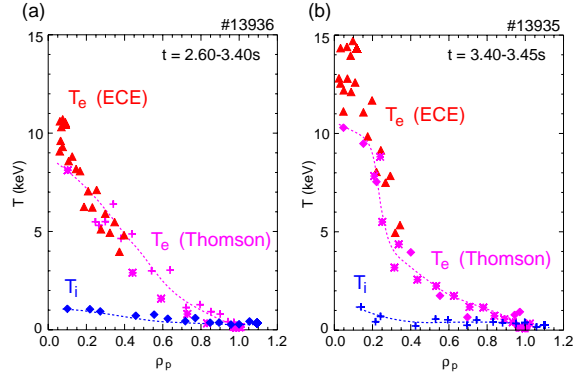
Associated with the reversed shear in the plasma center (figure 9) an internal transport barrier of the electron forms at $\rho_p \approx 0.3$ (figure 8(b)). In contrast to the co-ECCD case, where the central magnetic shear remains positive and q stays below one, the gradient length of the electron temperature profile decreases strongly. The possible necessity of reversed shear as a prerequisite of electron ITBs has been pointed out in previous experiments, ranging from regimes in which $T_e \gg T_i$ [28] to regimes with $T_e \approx T_i$ [29, 15, 30] or $T_e < T_i$ [10]. This is in qualitative agreement with recent theoretical considerations of electron temperature gradient (ETG) driven turbulence, which predict reduced electron heat transport in particular for low or reversed magnetic shear [31].
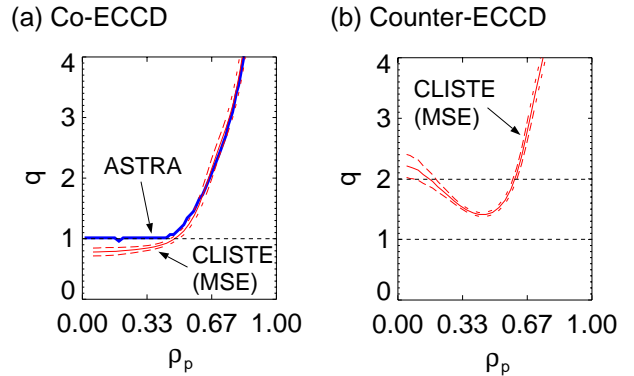

Figure 9. Safety factor profiles from ASTRA and CLISTE (with MSE): (a) co-ECCD, and (b) counter-ECCD phases.

5. Summary and conclusions

In ASDEX Upgrade, the negative central shear regime with L-mode edge has been extended to higher levels of heating power by using an upper SN configuration. Thus, ITBs with ion temperatures of the order of 15keV could be sustained for about 1s. The H-mode transition has to be avoided, since without a conducting wall the critical β_N for the destabilization of an external kink mode is exceeded in H-mode.

In high β_p plasmas fully non-inductive current drive with a fraction of bootstrap current of 56% and a neutral beam fraction of 44% has been achieved transiently. At $H_{ITER89-P}$=1.8, β_N=2.8, and β_p=3.1 Greenwald density is reached. The bootstrap current distribution suggests a shear reversal in the very plasma center.

In reversed shear plasmas with ion ITBs, the application of electron cyclotron resonance heating (ECRH) and current drive results in the formation of an additional electron barrier with $T_e \approx T_i$ without a deterioration of the ion or electron confinement [24, 15]. However, the strong pressure gradients of the combined electron and ion ITBs lead to infernal modes, which may be responsible for the disruptive termination of the discharges.

Central ECRH and current drive has been applied in low current and low density discharges. Current diffusion calculations, including the electron cyclotron current distribution calculated by a beam tracing code, predict that for co-ECCD a electron cyclotron current fraction of 82% has been reached. Together with 12% of bootstrap current this amounts to 94% of non-inductive current drive. In case of counter-ECCD, the central magnetic shear, which initially is positive with q_{min}<1, becomes negative and an electron ITB forms with a central T_e of about 10keV. As at low density only the electrons are heated directly, the ions remain cold (< 1keV). In contrast to the recent TCV results [7], the deposition was localized in the plasma center.

References

[1] LEVINTON, F. M. et al., Phys. Rev. Lett. **75** (1995) 4417.

[2] RICE, B. W. et al., Phys. Plasmas **3** (1996) 1983.

[3] FUJITA, T. et al., Plasma Phys. Control. Fusion **39** (1997) B75.

[4] SÖLDNER, F. X. et al., Nucl. Fusion **39** (1999) 407.

[5] GRUBER, O. et al., Nucl. Fusion **40** (2000) 1145.

[6] OIKAWA, T. et al., Nucl. Fusion **40** (2000) 435.

[7] SAUTER, O. et al., Phys. Rev. Lett. **84** (2000) 3322.

[8] KOIDE, Y. et al., Phys. Rev. Lett. **72** (1994) 3662.

[9] KAMADA, Y. et al., Nucl. Fusion **34** (1994) 1605.

[10]FUJITA, T. et al., Phys. Rev. Lett. **78** (1997) 2377.

[11]GRUBER, O. et al., Phys. Rev. Lett. **41** (1999) 1787.

[12]GÜNTER, S. et al., Nucl. Fusion **39** (1999) 1535.

[13]WOLF, R. C. et al., Plasma Phys. Control. Fusion **83** (1999) B93.

[14]WOLF, R. C. et al., Proc. 17th Int. Conf. on Plasma Physics and Controlled Fusion Research, IAEA-F1–CN-69/EXP1/12 (Yokohama 1998).

[15]WOLF, R. C. et al., Phys. Plasmas **7** (2000) 1839.

[16]MC CARTHY, P. J. et al., *The CLISTE Interpretive Equilibrium Code*, IPP-Report, IPP 5/85 (1999).

[17]WOLF, R. C. et al., Proc. 24th Eur. Conf. on Controlled Fusion and Plasma Physics, Berchtesgaden 1997, edited by R. Schittenhelm and R. Wagner, **Vol. 21A** (European Physical Society, Petit-Lancy, 1997) 1509.

[18]GÜNTER, S. et al., Nucl. Fusion **40** (2000) 1541.

[19]PEREVERZEV, G. et al., *ASTRA An Automatic System for Transport Analysis in a Tokamak*, IPP-Report, IPP 5/42 (1991).

[20]LIN, Z. et al., Phys. Plasmas **4** (1997) 1707.

[21]SHIANG, K. C. et al., Phys. Plasmas **4** (1997) 1375.

[22]PEREVERZEV, G. et al., Proc. 27th Eur. Conf. on Controlled Fusion and Plasma Physics, Budapest 2000 (European Physical Society, Petit-Lancy, 2000).

[23]LEUTERER, F. et al., *ECRH Experiments in ASDEX Upgrade*, submitted to Fusion Eng. Des. (1999).

[24]GÜNTER, S. et al., Phys. Rev. Lett. **84** (2000) 3097.

[25]POLI, E. et al., *A beam-tracing code for electron-cyclotron waves in tokamak plasmas* submitted to Computer Phys. Communications (2000).

[26]PEREVERZEV, G. V., Phys. Plasmas **5** (1998) 3529.

[27]KADOMTSEV, B. B., Sov. Journal of Plasma Physics **75** (1975) 389.

[28]BURATTI, P. et al., Phys. Rev. Lett. **82** (1999) 560.

[29]GÜNTER, S. et al., Nucl. Fusion **39** (1999) 1793.

[30]FOREST, C. B. et al., Phys. Rev. Lett. **77** (1996) 3141.

[31]JENKO, F. et al., Phys. Plasmas **7** (2000) 1904.